For a translationally invariant system

$$E_0 - W_0 = \frac{i}{2}\varsigma \int_0^1 \frac{d\lambda}{\lambda} \frac{\mathcal{V}}{(2\pi)^4} \int d^3k d\omega \sum_{\sigma\sigma'} \Sigma^\lambda_{\sigma\sigma'}(k,\omega) G^\lambda_{\sigma'\sigma}(k,\omega) e^{i\omega\eta} \quad . \tag{5.24b}$$

Analogous expressions for the Grand potential are obtained in terms of thermal Green's functions using the relation $\frac{d}{d\lambda}\Omega(\lambda) = \langle V \rangle$ proved in Problem 2.11 and the definition of the self energy Eq. (2.178) (note the sign)

$$\begin{aligned} \Omega - \Omega_0 &= \int_0^1 \frac{d\lambda}{\lambda} \langle \lambda V \rangle \\ &= \frac{1}{2}\varsigma \int \frac{d\lambda}{\lambda} \int dx \left[\left(-\frac{\partial}{\partial \tau} - T_x + \mu \right) \mathcal{G}(x\tau | x'\tau^+) \right]_{x=x'} \\ &= \frac{1}{2}\varsigma \int \frac{d\lambda}{\lambda} \int dx dx' d\tau' \Sigma^\lambda(x\tau | x'\tau') \mathcal{G}^\lambda(x'\tau' | x\tau^+) \quad . \end{aligned} \tag{5.25}$$

Note that the price of obtaining direct contact with diagrams is the additional parametric integral over the coupling strength λ.

It is an instructive to exercise to combine the diagrams for Σ and $\mathcal{G}$ to obtain the familiar expansion for $\Omega - \Omega_0$ or $E_0 - W_0$, and the details are given in Problem 5.1. The trace $\Sigma^\lambda \mathcal{G}^\lambda$ is represented by a closed graph composed of $\mathcal{G}^\lambda$ connecting to the two external points of Σ^λ. An n^{th} order contribution is obtained from an m^{th} order term of Σ^λ combined with an $(n-m)^{\text{th}}$ order term of $\mathcal{G}$ and the parametric integral yields a factor $\int_0^1 \frac{d\lambda}{\lambda}\lambda^n = \frac{1}{n}$. It is seen in Problem 5.1 that a given graph in $\Omega - \Omega_0$ arises from combinations of many bits and pieces of Σ^λ and $\mathcal{G}^\lambda$. Thus, the Grand potential is an example of a quantity which may often be more easily calculated directly rather than by using Green's functions. In addition to being inconvenient, use of the one-particle Green's function may also be dangerous since a seemingly innocuous approximation having little effect on one-particle properties may have a large uncontrolled effect on Ω. Physically, this reflects the fact that the one-particle Green's function is directly related to single-particle propagation in the many body system, instead of the two-body correlations to which E_0 and Ω_0 may be strongly sensitive. The principal results of this section are summarized in Table 5.1.

5.2 ANALYTIC PROPERTIES

Single-particle Green's functions have important analytic properties which follow from general principles. We will establish the salient properties of zero-temperature, real-time finite temperature, and thermal Green's functions in turn.

ZERO TEMPERATURE GREEN'S FUNCTIONS

The spectral representation for the zero-temperature Green's functions (Lehmann, 1954) is obtained by inserting a complete set of eigenstates between the field operators in the definition of $G(xt|x't')$, Eq. (5.3a).

$$\begin{aligned} iG(xt|x't') = &\sum_n \theta(t-t') \langle \psi_0 | \hat{\psi}(x,t) | \psi_n^{N+1} \rangle \langle \psi_n^{N+1} | \hat{\psi}^\dagger(x',t') | \psi_0 \rangle \\ &+ \varsigma \sum_n \theta(t'-t) \langle \psi_0 | \hat{\psi}^\dagger(x't') | \psi_n^{N-1} \rangle \langle \psi_n^{N-1} | \hat{\psi}(x,t) | \psi_0 \rangle \quad . \end{aligned} \tag{5.26}$$

$G(xt\|x't') = -i\langle\psi_0\|T\hat{\psi}(xt)\hat{\psi}^\dagger(x't')\|\psi_0\rangle$	$\mathcal{G}(x\tau\|x'\tau') = \frac{1}{\mathcal{Z}}\mathrm{Tr}\left(e^{-\beta(\hat{H}-\mu\hat{N})}T\hat{\psi}(xt)\hat{\psi}^\dagger(x't')\right)$
$\mathcal{G}_0^{-1} = i\frac{\partial}{\partial t} - H_0$	$\mathcal{G}_0^{-1} = \frac{\partial}{\partial \tau} + H_0 - \mu$
$\mathcal{G}^{-1} = i\frac{\partial}{\partial t} - H_0 - \Sigma$	$\mathcal{G}^{-1} = \frac{\partial}{\partial \tau} + H_0 - \mu + \Sigma$
$G(t) = \frac{1}{2\pi}\int d\omega\, e^{-i\omega t}\tilde{G}(\omega)$	$\mathcal{G}(\tau) = \frac{1}{\beta}\sum_{\omega_n} e^{-i\omega_n\tau}\tilde{\mathcal{G}}(\omega_0)$
$\tilde{G}_0(\omega) = \frac{1}{\omega - \epsilon_k + i\eta\,\mathrm{sgn}(\epsilon_k - \epsilon_F)}$	$\tilde{\mathcal{G}}_0(\omega_n) = \frac{-1}{i\omega_n - (\epsilon_k - \mu)}$
$\langle O\rangle = i\varsigma\int dx dx'\, O(x'x)G(xt\|x't^+)$	$\langle O\rangle = \varsigma\int dx dx'\, O(x'x)\mathcal{G}(x\tau\|x'\tau^+)$
$\hat{\psi}(x,t) = e^{i\hat{H}t}\hat{\psi}(x)e^{-i\hat{H}t}$	$\hat{\psi}(x,\tau) = e^{(\hat{H}-\mu\hat{N})\tau}\hat{\psi}(x)e^{-(\hat{H}-\mu\hat{N})\tau}$
$\hat{\psi}^\dagger(x,t) = e^{i\hat{H}t}\hat{\psi}^\dagger(x)e^{-i\hat{H}t}$	$\hat{\psi}^\dagger(x,\tau) = e^{(\hat{H}-\mu\hat{N})\tau}\hat{\psi}^\dagger(x)e^{-(\hat{H}-\mu\hat{N})\tau}$
$\langle H\rangle = \frac{1}{2}\varsigma\int dx\left[\left(i\frac{\partial}{\partial t}+T\right)G(xt\|x't^+)\right]_{x'=x}$	$\langle H\rangle = \frac{1}{2}\varsigma\int dx\left[\left(-\frac{\partial}{\partial \tau}+T+\mu\right)\mathcal{G}(x\tau\|x'\tau^+)\right]_{x=x'}$
$E-E_0 = \frac{1}{2}\varsigma\int_0^1\frac{d\lambda}{\lambda}\int dx\left[\left(i\frac{\partial}{\partial t}-T\right)G(xt\|x't^+)\right]_{x'=x}$	$\Omega-\Omega_0 = \frac{1}{2}\varsigma\int_0^1\frac{d\lambda}{\lambda}dx\left[\left(-\frac{\partial}{\partial \tau}-T+\mu\right)\mathcal{G}^\lambda(x\tau\|x'\tau^+)\right]_{x=x'}$
$= \frac{1}{2}\varsigma\int_0^1\frac{d\lambda}{\lambda}\int dx dx' dt' \Sigma^\lambda(xt\|x't')G^\lambda(x't'\|xt^+)$	$= \frac{1}{2}\varsigma\int_0^1\frac{d\lambda}{\lambda}\int dx dx' d\tau' \Sigma^\lambda(x\tau\|x'\tau')\mathcal{G}^\lambda(x'\tau'\|x\tau^+)$

Table 5.1 Summary of results for zero temperature and finite-temperature Green's Functions.

Note that the creation and annihilation operators only connect the N-particle ground state to $(N+1)$-particle states and $(N-1)$-particle states, respectively. The Heisenberg field operators acting on eigenstates $|\psi_n^M\rangle$ with energies E_n^M yield the explicit time-dependence $e^{-i(E_n^{N+1}-E_0)(t-t')}$ for the first term in Eq. (5.26) and $e^{-i(E_n^{N-1}-E_0)(t'-t)}$ for the second term. Using Eq. (3.30), the Fourier frequency transform of the Green's functions is

$$\begin{aligned} G(x,x';\omega) = &\sum_n \frac{\langle\psi_0|\hat{\psi}(x)|\psi_n^{N+1}\rangle\langle\psi_n^{N+1}|\hat{\psi}^\dagger(x')|\psi_0\rangle}{\omega - (E_n^{N+1}-E_0) + i\eta} \\ &- \varsigma\sum_n \frac{\langle\psi_0|\hat{\psi}^\dagger(x)|\psi_n^{N-1}\rangle\langle\psi_n^{N-1}|\hat{\psi}(x)|\psi_0\rangle}{\omega + (E_n^{N-1}-E_0) - i\eta} \quad . \end{aligned} \tag{5.27}$$

The analytic behavior of $G(\omega)$ has thus been clearly isolated and is sketched in Fig. 5.1. For each eigenstate $|\psi_n^{N+1}\rangle$ of the $(N+1)$-particle system, there is a pole in the lower half plane at $E^{N+1}-E_0$ with residue $\langle\psi_0|\hat{\psi}(x)|\psi_n^{N+1}\rangle\langle\psi_n^{N+1}|\hat{\psi}^\dagger(x)|\psi_0\rangle$ and for each eigenstate $|\psi_n^{N-1}\rangle$ there is a pole in the upper half plane at energy $-(E_n^{N-1}-E_0)$ with residue $\langle\psi_0|\hat{\psi}^\dagger(x)|\psi_n^{N-1}\rangle\langle\psi_n^{N-1}|\hat{\psi}(x)|\psi_0\rangle$. The poles in the lower half plane begin at $\mu^{N+1} = E_0^{N+1} - E_0$ and extend to $+\infty$ and those in the upper half plane extend from $-\infty$ up to $\mu^N = E_0 - E_0^{N-1}$. Because it is often convenient to deal with functions which are analytic in the upper or lower half plane, it is frequently useful to use the retarded and advanced Green's functions, Eq. (5.6). The analytic structure for

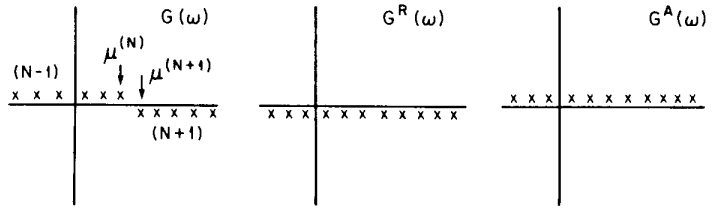

Fig. 5.1 Poles of $G(\omega)$, $G^R(\omega)$, and $G^A(\omega)$ in the complex ω plane.

$G^R_{(\omega)}$ and $G^A_{(\omega)}$ shown in Fig. 5.1 immediately follows from that of $G(\omega)$ by noting that $G^R(t-t')$ contains only $\theta(t-t')$ like the $(N+1)$-particle contribution to $G(t-t')$ and $G^A(t-t')$ contain $\theta(t'-t)$ like the $(N-1)$-particle contribution.

For notational simplicity, we will present the remaining results for a translationally invariant, infinite system. It is important to note, however, that all these results have obvious counterparts for finite systems. Since $\mu^{(N+1)} = \mu^{(N)} = \mu$ in the limit of large systems, it is convenient to measure all energies relative to the chemical potential and we define

$$\begin{aligned} E_n^{N+1} - E_0 &= E_n^{N+1} - E_0^{N+1} + E_0^{N+1} - E_0 \\ &\equiv \epsilon_n^{N+1} + \mu \end{aligned} \tag{5.28a}$$

and

$$\begin{aligned} E_n^{N-1} - E_0 &= E_n^{N-1} - E_0^{N-1} + E_0^{N-1} - E_0 \\ &\equiv \epsilon_n^{N-1} - \mu \quad . \end{aligned} \tag{5.28b}$$

Writing the field operator in momentum representation $\hat{\psi}(x) = \sum_k \frac{1}{\sqrt{\mathcal{V}}} e^{ik\cdot x}\hat{a}_k$ and writing eigenstates $\psi_n^{N\pm1}$ of total momentum $\pm k$, Fourier transformation of the Green's function Eq. (5.27) to momentum space yields

$$\left\{ \begin{matrix} G(\vec{k},\omega) \\ G^R(\vec{k},\omega) \\ G^A(\vec{k},\omega) \end{matrix} \right\} = \sum_n \left[\frac{|\langle \psi_n^{N+1}|a_k^\dagger|\psi_0\rangle|^2}{\omega - \mu - \epsilon_n^{N+1}\left\{ \begin{matrix} + \\ + \\ - \end{matrix} \right\} i\xi} - \varsigma \frac{|\langle \psi_n^{N-1}|a_k|\psi_0\rangle|^2}{\omega - \mu + \epsilon_n^{N+1}\left\{ \begin{matrix} - \\ + \\ - \end{matrix} \right\} i\xi} \right] \tag{5.29}$$

where we have now indicated the advanced and retarded cases as well for completeness. The two simplifications for infinite systems are positive definite residues, representing the probability of finding $a_k^\dagger|\psi_0\rangle$ or $a_k|\psi_0\rangle$ in eigenstates of the $(N+1)$- or $(N-1)$-particle systems, respectively, and a common starting point μ for the $(N+1)$- and $(N-1)$-particle poles. For real ω, Eq. (5.29) shows that G, G^R, and G^A are related as follows

$$G^R(\omega)^* = G^A(\omega) \tag{5.30}$$

and

$$G(\omega) = \begin{cases} G^R(\omega) & \omega > \mu \\ G^A(\omega) & \omega < \mu \end{cases} \tag{5.31a}$$

or equivalently

$$G(\omega) = G^R(\omega)\theta(\omega-\mu) + G^A(\omega)\theta(\mu-\omega) \quad . \tag{5.31b}$$

Since the poles of $G(k,\omega)$ become arbitrarily closely spaced in a large system, only averages can be measured and it is useful to define spectral weight functions

$$\begin{aligned} \rho^+(k,\omega) &= \sum_n |\langle \psi_n^{N+1}|a_k^\dagger|\psi_0\rangle|^2 2\pi\delta(\epsilon_n^{N+1} - \omega) \\ \rho^-(k,\omega) &= \sum_n |\langle \psi_n^{N-1}|a_k|\psi_0\rangle|^2 2\pi\delta(\epsilon_n^{N-1} - \omega) \end{aligned} \tag{5.32a}$$

and

$$\rho(k,\omega) = \theta(\omega)\rho^+(k,\omega) - \varsigma\theta(-\omega)\rho^-(k,-\omega) \quad . \tag{5.32b}$$

In terms of these weight functions,

$$G(k,\omega) = \int_0^\infty \frac{d\omega'}{2\pi}\left[\frac{\rho^+(k,\omega')}{\omega - \mu - \omega' + i\eta} - \varsigma\frac{\rho^-(k,\omega')}{\omega - \mu + \omega' - i\eta} \right] \tag{5.33a}$$

and

$$\begin{aligned} \left\{ \begin{matrix} G^R(k,\omega') \\ G^A(k,\omega') \end{matrix} \right\} &= \int_0^\infty \frac{d\omega'}{2\pi}\left[\frac{\rho^+(k,\omega')}{\omega - \mu - \omega' \pm i\eta} - \varsigma\frac{\rho^-(k,\omega')}{\omega - \mu + \omega' \pm i\eta} \right] \\ &= \int_{-\infty}^\infty \frac{d\omega'}{2\pi}\,\frac{\rho(k,\omega')}{\omega - \mu - \omega' \pm i\eta} \quad . \end{aligned} \tag{5.33b}$$

From the relation $\frac{1}{\omega \pm i\xi} = P\frac{1}{\omega} \mp i\pi\delta(\omega)$, where P is the principal part, it follows that

$$\begin{aligned} \mathrm{Re}\left\{ \begin{matrix} G(k,\omega) \\ G^R(k,\omega) \\ G^A(k,\omega) \end{matrix} \right\} &= P\int_{-\infty}^\infty \frac{d\omega'}{2\pi}\,\frac{\rho(k,\omega')}{\omega - \mu - \omega'} \quad , \\ \mathrm{Im}\left\{ \begin{matrix} G(k,\omega) \\ G^R(k,\omega) \\ G^A(k,\omega) \end{matrix} \right\} &= \left\{ \begin{matrix} -sgn(\omega-\mu) \\ - \\ + \end{matrix} \right\} \frac{1}{2}\rho(k,\omega-\mu) \end{aligned} \tag{5.34}$$

so that the Green's functions satisfy the dispersion relation

$$\mathrm{Re}\left\{ \begin{matrix} G(k,\omega) \\ G^R(k,\omega) \\ G^A(k,\omega) \end{matrix} \right\} = \frac{P}{\pi}\int_{-\infty}^\infty \frac{d\omega'}{\omega - \omega'} \left\{ \begin{matrix} -sgn(\omega'-\mu) \\ - \\ + \end{matrix} \right\} \mathrm{Im}\left\{ \begin{matrix} G(k,\omega) \\ G^R(k,\omega) \\ G^A(k,\omega) \end{matrix} \right\} \quad . \tag{5.35}$$

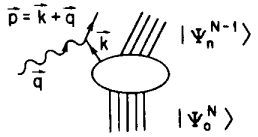

Fig. 5.2 Schematic representation of a (γ, p) or $(e, e'p)$reaction.

The commutation relations of the creation and annihilation operators give rise to a sum rule for the spectral weight

$$\begin{aligned} 1 = \langle\psi_0|\left[a_k, a_k^+\right]_{-\zeta}|\psi_0\rangle &= \sum_n |\langle\psi_n^{N+1}|a_k^+|\psi_0\rangle|^2 - \zeta\sum|\langle\psi_n^{N-1}|a_k|\psi_0\rangle|^2 \\ &= \int_0^\infty \frac{d\omega}{2\pi}\left[\rho^+(k,\omega) - \zeta\rho^-(k,\omega)\right] \\ &= \int_{-\infty}^\infty \frac{d\omega}{2\pi}\rho(k,\omega) \quad . \end{aligned} \tag{5.36}$$

Combined with Eqs. (5.33), this sum rule establishes the high frequency behavior of the Green's functions:

$$\left\{\begin{matrix} G(\omega) \\ G^R(\omega) \\ G^A(\omega) \end{matrix}\right\} \underset{\omega\to\infty}{\longrightarrow} \int_0^\infty \frac{d\omega'}{2\pi}\,\frac{\rho^+(k,\omega') - \zeta\rho^-(k,\omega')}{\omega} = \frac{1}{\omega} \quad . \tag{5.37}$$

Experimentally, the spectral weight function is accessible through semi-inclusive experiments. Consider, for example, a (γ, p) or $(e, e'p)$ reaction on a nucleus, as sketched in Fig. 5.2 in which a real or virtual photon of momentum q is absorbed by a nucleus in its ground state $|\psi_0\rangle$ and a proton is ejected. In the final state, only the ejected proton having momentum $p = k + q$ is detected and the rest of the state is unresolved. In the impulse approximation, (in which the interactions of the ejected particles are neglected) the proton knocked out by the photon must have had an initial momentum of k, so a proton of momentum k has been removed and the cross section is

$$\begin{aligned} \sigma &= 2\pi\sum|\langle\psi_n^{N-1}|a_k|\psi_0\rangle|^2\delta(E_n^{N-1} + E_p - E_0 - E_\gamma) \\ &= \rho^-(k, E_\gamma + \mu^N - E_\rho) \quad . \end{aligned} \tag{5.38}$$

By varying the kinematics and including corrections to the impulse approximation, much has been learned about the behavior of the spectral weights (Frullani and Mougey, 1984). An interesting energy weighted sum rule for $\rho^-(k,\omega)$ has been derived by Koltun (1972) and is derived in Problem 5.2.

FINITE TEMPERATURE GREEN'S FUNCTIONS

We now turn our attention to the analytic properties of finite-temperature Green's functions. Instead of regarding thermal and real-time Green's functions, Eq. (5.1–5.2),

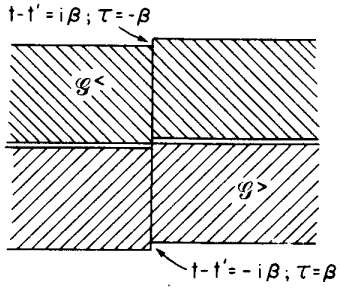

Fig. 5.3 Domains of complex $t - t'$ plane in which $\mathcal{G}^>(xt|x't')$ and $\mathcal{G}^<(xt|x't')$ may be continued. By the periodicity of $\mathcal{G}$, the domains are reported indefinitely in the imaginary t direction.

as distinct entities, it is useful to consider $\mathcal{G}(xt|x't')$ as a function in the complex $t-t'$ plane. Under the change of variables $it \to \tau$,

$$\begin{aligned} \hat\psi(x,t) = e^{it(\hat H-\mu\hat N)}\hat\psi(x)e^{-it(H-\mu\hat N)} &\to e^{\tau(\hat H-\mu\hat N)}\hat\psi(x)e^{-\tau(\hat H-\mu\hat N)} = \hat\psi(x,\tau) \\ \hat\psi^\dagger(x,t) &\to \hat\psi^\dagger(x,\tau) \end{aligned} \tag{5.39a}$$

so that

$$i\mathcal{G}(xt|x't') \to \mathcal{G}(x\tau|x'\tau') \tag{5.39b}$$

Thus, a single function of a complex time variable specifies the real time Green's function along the real-t-axis and the thermal Green's functions along the imaginary t-axis. The real-time Green's function, which describes the physical response of a system, may thereby be obtained from the thermal Green's function, which is calculable by the perturbation theory described in Chapter 2, by straightforward analytic continuation. To see the analytic structure of $\mathcal{G}$ in the complex t-plane, we write

$$\mathcal{G}(xt|x't') = \theta(t-t')\mathcal{G}^>(xt|x't'|) + \theta(t'-t)\mathcal{G}^<(xt|x't) \tag{5.40a}$$

where

$$\begin{aligned} \mathcal{G}^>(xt|x't') &= \frac{-i}{Z}\mathrm{Tr}\left\{e^{-(\beta-i(t-t'))(\hat H-\mu\hat N)}\hat\psi(x)e^{-i(t-t')(\hat H-\mu\hat N)}\hat\psi^\dagger(x')\right\} \\ \mathcal{G}^<(xt|x't') &= \frac{-\zeta i}{Z}\mathrm{Tr}\left\{e^{-(\beta+i(t-t'))(\hat H-\mu\hat N)}\hat\psi^\dagger(x')e^{i(t-t')(\hat H-\mu\hat N)}\hat\psi(x)\right\} \end{aligned} \tag{5.40b}$$

In order for the thermodynamic traces to converge, $\mathcal{G}^>$ and $\mathcal{G}^<$ can only be continued into regions in which the factors multiplying $\hat H - \mu\hat N$ in the exponentials have negative real parts. (Note that $\hat H - \mu\hat N$ must be positive for the partition function to exist). Hence, $\mathcal{G}^>(t-t')$ can be continued if $\mathrm{Re}\{\beta - i(t-t')\} > 0$ and $\mathrm{Re}\{i(t-t')\} > 0$. Similarly, $\mathcal{G}^<(t-t')$ can be continued if $\mathrm{Re}\{\beta + i(t-t')\} > 0$ and $\mathrm{Re}\{i(t-t')\} < 0$. Thus, $\mathcal{G}^>$ and $\mathcal{G}^<$ may be continued from the real axis in the following domains, which are also sketched in Fig. 5.3.

$$\begin{aligned} -\beta < \mathrm{Im}(t-t') < 0 \quad & G^>(t-t') \\ 0 < \mathrm{Im}(t-t') < \beta \quad & G^<(t-t') \quad . \end{aligned} \tag{5.41}$$

We have already shown in Chapter 2 that thermal Green's functions for the non-interacting system are periodic or antiperiodic with period β. Thus, the interacting $\mathcal{G}$ constructed from them must also be periodic or antiperiodic when the imaginary part of the argument is shifted by β, and we confirm that $G^<(t-t')$ is related to $G^>(t-t'-i\beta)$ appropriately as follows, using Eq. (5.40) and the cyclic property of the trace:

$$\begin{aligned} G^<(x,x';(t-t')) &= \frac{-i\varsigma}{Z}\mathrm{Tr}\left\{e^{i(t-t')(\hat{H}-\mu\hat{N})}\hat{\psi}(x)e^{-(\beta+i(t-t'))(\hat{H}-\mu\hat{N})}\hat{\psi}^\dagger(x')\right\} \\ &= \varsigma\left[\frac{-i}{Z}\mathrm{Tr}\left\{e^{-(\beta-i(t-t'-i\beta))(\hat{H}-\mu\hat{N})}\hat{\psi}(x)e^{-i(t-t'-i\beta)(\hat{H}-\mu\hat{N})}\psi^\dagger(x')\right\}\right] \\ &= \varsigma G^>(x,x';(t-t'-i\beta)) \quad . \end{aligned} \tag{5.42}$$

This periodicity is consistent with the domain of continuation shown in Fig. 5.3, since the discontinuity between $G^>$ and $G^<$ adjacent to the real axis must be repeated again along the $t-t'=\pm i\beta$ axes.

To study the analytic properties in the ω plane, we insert a complete set of states to extract the explicit time dependence as in the zero-temperature case and Fourier transform. As before, the singularity structure is the same for finite and translationally invariant systems, and we only treat the translationally invariant case here for notational convenience. Writing the trace and completeness relation using a complete set of eigenstates $\{|\psi_m\rangle\}$ with all number of particles

$$\begin{aligned} i\mathcal{G}(xt|x't') = {} & \theta(t-t')\frac{1}{Z}\sum_{m,n}\langle\psi_m|e^{-\beta(H-\mu N)}\hat{\psi}(x,t)|\psi_n\rangle\langle\psi_n|\hat{\psi}^\dagger(x't')|\psi_m\rangle \\ & + \varsigma\theta(t'-t)\frac{1}{Z}\sum_{m,n}\langle\psi_n|e^{-\beta(H-\mu N)}\hat{\psi}^\dagger(x',t')|\psi_m\rangle\langle\psi_m|\hat{\psi}(x,t)|\psi_n\rangle \quad . \end{aligned} \tag{5.43}$$

Extracting the time dependence as in Eq. (5.26), Fourier transforming to frequency and momentum space as in Eqs. (5.27) and (5.29) and treating the advanced and retarded cases in the same way, we obtain

$$\begin{aligned} \begin{Bmatrix} G(k,\omega) \\ G^R(k,\omega) \\ G^A(k,\omega) \end{Bmatrix} = {} & \frac{1}{Z}\sum_{m,n}|\langle\psi_n|a_k^\dagger|\psi_m\rangle|^2 \\ & \times\left\{\frac{e^{-\beta(E_m-\mu N_m)}}{\omega-(E_n-E_m-\mu)\begin{Bmatrix}+\\+\\-\end{Bmatrix}i\eta} - \varsigma\frac{e^{-\beta(E_n-\mu N_n)}}{\omega-(E_n-E_m-\mu)\begin{Bmatrix}-\\+\\-\end{Bmatrix}i\eta}\right\} \quad . \end{aligned} \tag{5.44}$$

Note that we have used the fact that the only non-vanishing contributions arise for states in which the number of particles in state n, N_n, is one larger than the number in m, N_m. Since the two terms in Eq. (5.44) include all $N_n = N_m + 1$, they have a more symmetrical form than the corresponding terms in Eq. (5.2.4) which involve only $N+1$ and $N-1$. Thus, we may combine them to write the spectral weight function as

$$\begin{aligned} \rho(k,\omega) = \frac{1}{Z}\sum_{m,n}\Big\{ & \left|\langle\psi_n|a_k^\dagger|\psi_m\rangle\right|^2 e^{-\beta(E_m-\mu N_m)}(1-\varsigma e^{-\beta\omega}) \\ & \times 2\pi\delta[E_n-E_m-\mu-\omega]\Big\} \quad . \end{aligned} \tag{5.45}$$

One observes that this expression effectively reduces to Eq. (5.32b) in the zero temperature limit as follows. For $\omega > 0$ the first term dominates and denoting by m_0 the state with minimum $E_m - \mu N_m$, $\lim_{\beta\to\infty}\frac{1}{Z}\sum_m e^{-\beta(E_m-\mu N_m)}|\langle\psi_n|a_k^\dagger|\psi_m\rangle|^2 = \langle\psi_n|a_k^\dagger|\psi_{m_0}\rangle|^2$. Analogously, for $\omega < 0$, the second term dominates and yields the factor $|\langle\psi_{m_0}|a_k^\dagger|\psi_n\rangle|^2$.

Using Eq. (5.45), the spectral representation of $\mathcal{G}^R$ and $\mathcal{G}^A$ may be written in the same form as the zero-temperature case, Eq. (5.33b).

$$\begin{Bmatrix} \mathcal{G}^R(k,\omega) \\ \mathcal{G}^A(k,\omega) \end{Bmatrix} = \int_{-\infty}^{\infty}\frac{d\omega'}{2\pi}\,\frac{\rho(k,\omega')}{\omega-\omega'\pm i\eta} \quad . \tag{5.46}$$

The real and imaginary parts obtained from Eq. (5.44) and (5.46) may be expressed in the following form using the identity $1+\eta e^{-\beta\omega} = \tanh\left(\frac{\beta u}{2}\right)^{-\eta}(1-\varsigma e^{-\beta\omega})$

$$\begin{aligned} \mathrm{Re}\begin{Bmatrix} \mathcal{G}(k,\omega) \\ \mathcal{G}^R(k,\omega) \\ \mathcal{G}^A(k,\omega) \end{Bmatrix} &= P\int_{-\infty}^{\infty}\frac{d\omega'}{2\pi}\,\frac{\rho(k,\omega')}{\omega-\omega'} \\ \mathrm{Im}\begin{Bmatrix} \mathcal{G}(k,\omega) \\ \mathcal{G}^R(k,\omega) \\ \mathcal{G}^A(k,\omega) \end{Bmatrix} &= \begin{Bmatrix} -\tanh\left(\frac{\beta\omega}{2}\right)^{-\varsigma} \\ - \\ + \end{Bmatrix}\frac{1}{2}\rho(k,\omega) \quad . \end{aligned} \tag{5.47}$$

Hence, we obtain the dispersion relations

$$\mathrm{Re}\begin{Bmatrix} \mathcal{G}(k,\omega) \\ \mathcal{G}^R(k,\omega) \\ \mathcal{G}^A(k,\omega) \end{Bmatrix} = \frac{P}{\pi}\int_{-\infty}^{\infty}\frac{d\omega'}{\omega-\omega'}\begin{Bmatrix} -\tanh\left(\frac{\beta\omega}{2}\right)^{-\varsigma} \\ - \\ + \end{Bmatrix}\rho(k,\omega) \tag{5.48}$$

and the relation between $\mathcal{G}$, $\mathcal{G}^R$, and $\mathcal{G}^A$

$$\begin{aligned} \mathcal{G}(k,\omega) &= \frac{\mathcal{G}^R(k,\omega)}{1-\varsigma e^{-\beta\omega}} + \frac{\mathcal{G}^A(k,\omega)}{1-\varsigma e^{\beta\omega}} \\ &= 1+\varsigma n(\omega+\mu)\mathcal{G}^R(k,\omega) - \varsigma n(\omega+\mu)\mathcal{G}^A(k,\omega) \end{aligned} \tag{5.49}$$

where $n(\omega+\mu)$ is the familiar occupation probability, Eq. (2.75b). The last result reflects the fact that the poles in the upper and lower half plane overlap at finite

temperature and only in the zero temperature limit does one recover the simple structure of non-overlapping poles reflected in Eq. (5.34b):

$$\mathcal{G}(k,\omega) \underset{\beta\to\infty}{\longrightarrow} \theta(\omega)\mathcal{G}^R(k,\omega) + \theta(-\omega)\mathcal{G}^A(k,\omega) \quad . \tag{5.50}$$

Note in making this comparison that at finite temperature the combination $\omega+\mu$ occurred in Eq. (5.44) where only the frequency occurred at zero temperature in Eq. (5.27). Denoting the zero-temperature convention for the frequency as $\omega_0 = \omega+\mu$, we confirm that the factors $\theta(\pm\omega) = \theta(\pm(\omega_0-\mu))$ agree with Eq. (5.31b). The sum rule for $\rho(k,\omega)$ is obtained as in Eq. (5.36).

$$1 = \frac{1}{2}\mathrm{Tr}\{e^{-\beta(\hat{H}-\mu\hat{N})}[a_k, a_k^\dagger]_{-\varsigma}\} = \int_{-\infty}^{\infty}\frac{d\omega}{2\pi}\rho(k,\omega) \tag{5.51}$$

so that the finite temperature Green's functions have the high frequency behavior

$$\left\{\begin{array}{c}\mathcal{G}(k,\omega)\\ \mathcal{G}^R(k,\omega)\\ \mathcal{G}^A(k,\omega)\end{array}\right\} \underset{\omega\to\infty}{\longrightarrow} \int\frac{d\omega'}{2\pi}\,\frac{\rho(k,\omega')}{\omega} = \frac{1}{\omega} \quad . \tag{5.52}$$

Finally, we relate the thermal Green's function to the real-time Green's function through its spectral representation. Since $\mathcal{G}(x,x';\,\tau-\tau')$ is periodic or antiperiodic on the interval $(0,\,\beta)$, we expand in a Fourier series with Matsubara frequencies $\omega_n = \frac{2n\pi}{\beta}$ or $\frac{(2n+1)\pi}{\beta}$ defined in Eq. (3.129). Inserting a complete set of states in $\mathcal{G}(x\tau|x'0)$, Eq. (5.2), and evaluating the Fourier transform on the interval $0<\tau<\beta$ as in Eq. (2.131) yields

$$\begin{aligned}\mathcal{G}(k,\omega_s) &= \frac{1}{Z}\int_0^\beta d\tau\, e^{i\omega_s\tau}\sum_{mn}|\langle\psi_n|a_k^\dagger|\psi_m\rangle|^2\, e^{\tau[E_m-E_n+\mu]}\, e^{-\beta(E_m-\mu N_m)}\\ &= \frac{1}{Z}\sum_{mn}|\langle\psi_n|a_k^\dagger|\psi_m\rangle|^2\, e^{-\beta(E_m-\mu N_m)}\left[\frac{-1+\varsigma\, e^{-\beta(E_n-E_m-\mu)}}{i\omega_s-(E_n-E_m-\mu)}\right]\\ &= -\int_{-\infty}^{\infty}\frac{d\omega'}{2\pi}\,\frac{\rho(k,\omega')}{i\omega_s-\omega'} \quad .\end{aligned} \tag{5.53}$$

Comparison with Eq. (5.46) shows that $-\mathcal{G}(k,\omega_n)$, $\mathcal{G}^R(k,\omega_n)$ and $\mathcal{G}^A(k,\omega_n)$ are given by the same complex function specified by the weight $\rho(k,\omega)$ evaluated along the imaginary axis at the discrete Matsubara frequencies or infinitesimally above or below the real axis. Given the positions of the singularities of $\mathcal{G}^R$ and $\mathcal{G}^A$ sketched in Fig. 5.4, it is clear that $-\mathcal{G}(\omega_n)$ calculated in perturbation theory is to be continued in the upper half plane to determine $\mathcal{G}^R$ and in the lower half plane to determine $\mathcal{G}^A$. From $\mathcal{G}^R(\omega)$ and $\mathcal{G}^A$, $\mathcal{G}(\omega)$ is specified by Eq. (5.49). Although perturbation theory only specifies $\mathcal{G}(\omega_n)$ at a discrete set of points, the continuation is unique because of the requirement that $\mathcal{G}(\omega)\sim\frac{1}{|\omega|}$ at infinity.

Although we will subsequently present a detailed example of how this analytic continuation works in Section 5.5, we conclude this present section with the simple

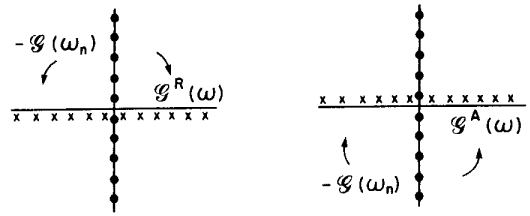

Fig. 5.4 Continuation of the function $\int\frac{d\omega'}{2\pi}\,\frac{\rho(\omega')}{\omega-\omega'}$ in the complex ω plane from points $\omega = i\omega_n$ along the imaginary axis where it equals $-\mathcal{G}(\omega_n)$ to points infinitesimally above the real axis where it yields $\mathcal{G}^R(\omega)$ and below the real axis where it gives $\mathcal{G}^A(\omega)$.

example of the Green's function for a non-interacting system. Equating the non-interacting thermal Green's functions, Eq. (2.131b) to the spectral representation Eq. (5.53), we obtain

$$\frac{-1}{i\omega_n-(\epsilon_k-\mu)} = -\int\frac{d\omega'}{2\pi}\,\frac{\rho(k,\omega')}{i\omega_n-\omega'} \tag{5.54a}$$

from which it follows that

$$\rho(k,\omega') = 2\pi\delta\left[\omega'-(\epsilon_k-\mu)\right] \tag{5.54b}$$

$$\left\{\begin{array}{c}\mathcal{G}^R(k,\omega)\\ \mathcal{G}^A(k,\omega)\end{array}\right\} = \int\frac{d\omega'}{2\pi}\,\frac{\rho(k,\omega')}{\omega-\omega'\pm i\eta} = \frac{1}{\omega-(\epsilon_k-\mu)\pm i\eta} \quad . \tag{5.54c}$$

These manipulations are equivalent to simply replacing $i\omega_n$ in the thermal Green's function by $\omega\pm i\eta$ in the real-time Green's function (and including the overall minus sign from our conventions). Since there is only a single pole, there is no distinction between continuation from above or below the real axis. By Carlson's theorem, other functions, such as $\frac{e^{\beta\omega}}{\omega-(\epsilon_k-\mu)\pm i\eta}$ or $\frac{1}{\omega-(\epsilon_k-\mu)\pm+i\eta}+\sin\beta\omega$ which coincide with the thermal Green's function at the points $i\omega_n$ are ruled out because they do not converge as $\frac{1}{|\omega|}$ at large ω. Thus, shifting the frequency by μ to coincide with the zero-temperature convention and using Eq. (5.49) we obtain

$$\begin{aligned}\mathcal{G}(k,\omega-\mu) &= (1+\varsigma n(\omega))\,\mathcal{G}^R(\omega-\mu) - \varsigma n(\omega)\mathcal{G}^A(\omega-\mu)\\ &= \frac{1+\varsigma n(\epsilon_k)}{\omega-\epsilon_k+i\eta} - \frac{\varsigma n(\epsilon_k)}{\omega-\epsilon_k-i\eta}\end{aligned} \tag{5.55}$$

consistent with the zero temperature limit, Eq.(3.31)

5.3 PHYSICAL CONTENT OF THE SELF ENERGY

At this point, it is appropriate to complement the treatment of the formal properties of Green's functions by considering the physical content of a specific illustrative case: the one-particle Green's function for Fermions at zero temperature. Since

Dyson's equation, Eq.(2.178) expresses the difference between the non-interacting and interacting Green's functions in terms of the self-energy, Σ

$$G_0(k,\omega) = \frac{1}{\omega - \epsilon_k + i\xi \mathrm{sgn}(\omega)} \tag{5.56}$$

$$G(k,\omega) = \frac{1}{\omega - \epsilon_k - \Sigma(k,\omega)} \tag{5.57}$$

all the many-body physics is contained in Σ and it is most convenient to study $\Sigma(k,\omega)$ directly. Recall the convention from Chapter 3 that all energies and frequencies are defined relative to the Fermi energy ϵ_F. Also note once again that we assume translational invariance not of physical necessity but rather to simplify the notation by rendering equations diagonal in momentum space.

The essential features of Σ arise in the first two orders of perturbation theory, so we shall consider the approximate Green's function defined by the second order self-energy

$$G_2(k,\omega) = \frac{1}{\omega - \epsilon_k - \Sigma_1(k) - \Sigma_2(k,\omega)} \ . \tag{5.58}$$

The first-order self-energy is

$$\Sigma_1(\alpha) = $$ 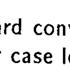 $$= \sum_A \{\alpha A|v|\alpha A\} \tag{5.59}$$

where, according to our standard conventions, the curly brackets denote an antisymmetrized matrix element, upper case letters denote occupied momentum states, lower case letters denote unoccupied momentum states, and the Greek letters (with the exception of ω which always denotes frequency) indicate an unrestricted momentum which may be above or below k_F. Because the eigenfunctions in a translationally invariant system are plane waves, $\Sigma_1(\alpha)$ coincides with the Hartree Fock potential, Eq. (2.180). Note that since the Hartree-Fock potential is instantaneous, it has no frequency dependence. The full generality of the structure in the self-energy arises in second order, for which we have previously evaluated the contributions of diagrams having two-particle one-hole intermediate states and two-hole one-particle intermediate states, Eqs. (3.58 – 3.59):

$$\Sigma_2^{2p1h}(\alpha,\omega) = $$ 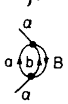 $$= \frac{1}{2}\sum_{abB} \frac{|\{\alpha B|v|ab\}|^2}{\omega + \epsilon_B - \epsilon_a - \epsilon_b + i\eta}$$

$$\Sigma_2^{2h1p}(\alpha,\omega) = $$  $$= -\frac{1}{2}\sum_{ABb} \frac{|\{\alpha b|v|AB\}|^2}{\epsilon_A + \epsilon_B - \epsilon_a - \omega + i\eta} \ . \tag{5.60}$$

Because these and all higher order diagrams have finite extent in time, they have explicit frequency dependence.

Both terms in Σ_2 have an infinite number of poles. The denominator of Σ^{2p1h} vanishes when $\omega = \epsilon_a + \epsilon_b - \epsilon_B$ which requires ω positive corresponding to an energy greater than ϵ_F. Similarly, Σ^{2h1p} has poles when $\omega = \epsilon_A + \epsilon_B - \epsilon_a$ corresponding to ω negative and energies less than ϵ_F. Since $\mathrm{Im}\,\Sigma^{2p1h} < 0$ and $\mathrm{Im}\,\Sigma^{2h1p} > 0$, the finite imaginary parts of Σ_2 replace the infinitesimal displacement $i\eta\,\mathrm{sgn}(\omega)$ required in the non-interacting Green's function.

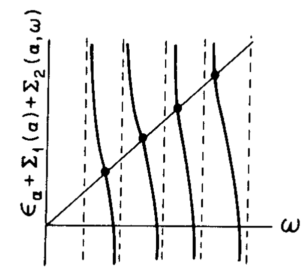

Fig. 5.5 Sketch of $\epsilon_\alpha + \Sigma_1(\alpha) + \Sigma_2(\alpha,\omega)$ as a function of ω. The dashed vertical asymptotes denote the poles of $\Sigma_2(\alpha,\omega)$ and the dots indicate the graphical solutions for the positions of the poles in $G_2(\alpha,\omega)$.

QUASIPARTICLE POLE

We now consider the poles in $G_2(\alpha,\omega)$. By our general arguments in Section 5.2, the poles represent the eigenstates of the interacting $N+1$ particle system and the residues specify their overlap with $a_\alpha^\dagger|\psi_0\rangle$. If the system behaves as non-interacting particles, there will be a single pole with unit strength as in the case of $\mathcal{G}_0(\alpha,\omega)$. As the system becomes more and more strongly interacting, the strength will become fragmented between more and more complicated states, subject only to the sum rule that the integrated strength remains 1.

To analyze the pole structure of $G_2(\alpha,\omega)$, it is convenient to perform the graphical construction shown in Fig. 5.5, where $\epsilon_\alpha + \Sigma_1(\alpha) + \Sigma_2(\alpha,\omega)$ is sketched as a function of ω. We will first consider states above the Fermi sea. For every value $\omega = \epsilon_a + \epsilon_b - \epsilon_B$ at which $\Sigma_2^{2p1h}(\alpha,\omega)$ has a pole, a vertical asymptote is drawn in Fig. 5.5, and the function $\epsilon_\alpha + \Sigma_1(\alpha) + \Sigma_2^{2p1h}(\alpha,\omega)$ must smoothly decrease from $+\infty$ to $-\infty$ between even pair of asymptotes as shown. The condition for a pole in $G_2(\alpha,\omega)$ that $\omega = \epsilon_\alpha + \Sigma_1(\alpha) + \Sigma_2^{2p1h}(\alpha,\omega)$ is represented on the graph by the intersection of $\epsilon_\alpha + \Sigma_1(\alpha) + \Sigma_2^{2p1h}(\alpha,\omega)$ with the straight line at 45°.

Having appreciated the general structure, it is instructive to consider a schematic example. Instead of the infinite number of poles discussed above, we will assume $\Sigma_2(\omega)$ has only two poles

$$\Sigma_2(\omega) = \frac{A_1}{\omega - E_1} + \frac{A_2}{\omega - E_2} \tag{5.61}$$

and study the poles and residues of

$$G_2(\omega) = \frac{1}{\omega - E_0 - \Sigma_2(\omega)} \tag{5.62}$$

where for notational convenience $E_0 = \epsilon_\alpha + \Sigma_1$ and we have suppressed the $i\eta$. Further, we will assume that E_1 is above E_0, E_2 is below E_0 and that the residues in Σ_2 are very small, satisfying the conditions

$$\frac{A_i}{|E_i - E_0|\,|E_j - E_0|} < \delta << 1 \qquad \begin{array}{l} i = 1,2 \\ j = 1,2 \end{array} \ . \tag{5.63}$$

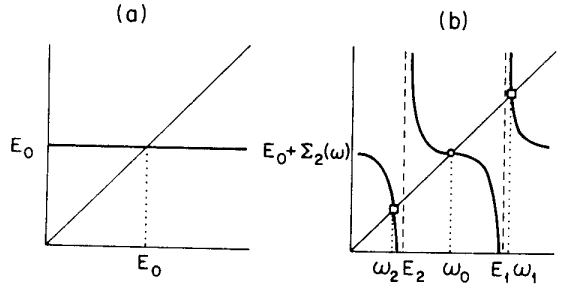

Fig. 5.6 Graphical solution for the poles of $G_1(\omega)$ and $G_2(\omega)$ in Eqs. (5.62) and (5.64).

For subsequent reference, since A_1 and A_2 are very weak so that $\Sigma_2(\omega)$ is in some sense small, we first neglect $\Sigma_2(\omega)$ entirely and perform the graphical construction for

$$G_1(\omega) = \frac{1}{\omega - E_0} \tag{5.64}$$

in part (a) of Fig. 5.6. Since E_0 has no ω-dependence, the graph is structureless and a single pole of unit residue occurs at E_0. In part (b) of Fig. 5.6, the graphical construction is repeated for $G_2(\omega)$. Far away from E_1 and E_2, $E_0+\Sigma_2(\omega)$ approaches the horizontal line sketched in part (a), and it is only very close to the singularities E_1 and E_2 that the curve diverges to $\pm\infty$. Instead of the single pole at E_0 in case (a), we now have three poles: ω_1 very close to E_1, ω_2 close to E_2, and ω_0 close to E_0.

We now expand $G_2(\omega)$ around each of the three poles ω_s which are solutions to the equation

$$\omega_s = E_0 + \Sigma_2(\omega_s) \qquad s = 0,\ 1,\ 2\ . \tag{5.65}$$

Near the pole ω_s,

$$\begin{aligned} \omega - E_0 - \Sigma_2(\omega) &\approx \omega - E_0 - \Sigma_2(\omega_s) - (\omega - \omega_s)\Sigma_2'(\omega_s) \\ &= (\omega - \omega_s)\,(1 - \Sigma_2'(\omega_s)) \end{aligned} \tag{5.66a}$$

so that

$$G_2(\omega) \approx \frac{1}{(1 - \Sigma_2'(\omega_s))}\,\frac{1}{\omega - \omega_s}\ . \tag{5.66b}$$

Thus, in general the residue of each pole is $\frac{1}{1-\Sigma_2'(\omega_s)}$. For our schematic model, the assumption (5.63) makes it easy to evaluate the residue for each pole.

First, note using Eqs. (5.65) and (5.63) that the shifts $\omega_s - E_s$ are negligible relative to the energy spacing and

$$\begin{aligned} (\omega_i - E_0) &= (E_i - E_0)\,(1 + \mathcal{O}(\delta)) \qquad i = 1, 2 \\ (E_i - \omega_0) &= (E_i - E_0)\,(1 + \mathcal{O}(\delta)) \\ (\omega_i - E_0) &= \left(\frac{A_i}{\omega_i - E_i}\right)(1 + \mathcal{O}(\delta))\ . \end{aligned} \tag{5.67}$$

To leading order in δ, the residues are

$$\begin{aligned} \frac{1}{1 - \Sigma_2'(\omega_0)} &= \frac{1}{1 + \sum_{i=1}^{2} \frac{A_i}{(\omega_0 - E_i)^2}} \\ &\approx \frac{1}{1 + \sum_{i=1}^{2} \frac{A_i}{(E_0 - E_i)^2}} \\ &\approx 1 - \sum_{i=1}^{2} \frac{A_i}{(E_0 - E_i)^2} \end{aligned} \tag{5.68a}$$

and

$$\begin{aligned} \frac{1}{1 - \Sigma_2'(\omega_i)} &= \frac{1}{1 + \sum_{j=1}^{2} \frac{A_j}{(\omega_i - E_j)^2}} \\ &\approx \frac{1}{1 + \frac{(\omega_i - E_0)^2}{A_i}} \\ &\approx \frac{A_i}{(E_0 - E_i)^2} \qquad i = 1,\ 2\ . \end{aligned} \tag{5.68b}$$

Now, the full physical effect of switching on the matrix elements A_i is evident. Without this coupling, the system has a pole with unit residue corresponding to the propagation of a single particle, as sketched in Fig. 5.6a. After switching on the interaction, Fig. 5.6b, the strength is now fragmented between three poles. The system still possesses a fundamental excitation near the original energy E_0, but now the energy is shifted slightly to ω_0 and the residue $1 - \sum_{i=1}^{2} \frac{A_i}{(E_0 - E_i)^2}$ is less than one. This pole is called the quasiparticle pole: it still behaves very much like a single-particle excitation, but is no longer a true particle pole because of the medium modifications. Consistent with the sum rule, Eq. (5.36), the strength which has been removed from the quasiparticle pole has been distributed to the two new poles, with strength $\frac{A_i}{(E_0 - E_i)^2}$ going to the pole at ω_i. These poles represent more complicated excitations of the many-particle medium, such as two-particle, one hole states.

With this schematic model as an introduction, it is now appropriate to return to the general expression for the second-order self-energy, Eq. (5.60), which has both two-particle one-hole and two-hole one-particle contributions. The residue of the quasiparticle pole corresponding to the state α, assuming a weak interaction v, is given by

$$\frac{1}{1 - \frac{\partial}{\partial\omega}\Sigma_2(\alpha, \omega)} \approx 1 - \frac{1}{2}\sum_{abB} \frac{|\{\alpha B|v|ab\}|^2}{(\omega + \epsilon_B - \epsilon_a - \epsilon_b)^2} - \frac{1}{2}\sum_{ABb} \frac{|\{\alpha b|v|AB\}|^2}{(\epsilon_A + \epsilon_B - \epsilon_a - \omega)^2}. \tag{5.69}$$

Thus, as shown in Fig. 5.7, the strength associated with a particle state is depleted by coupling both to two-particle one-hole states above the Fermi surface and to two-hole one-particle states below the Fermi surface. In the limit of a continuum, these two-particle one-hole and two-hole one-particle states yield a smooth background in addition to the simple quasiparticle excitations.

Having introduced quasiparticles, it is natural to ask if there is any regime in which they provide a useful and accurate description of a physical system or whether

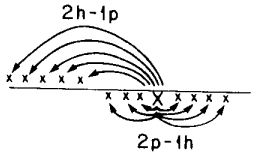

Fig. 5.7 Fragmentation of strength of the quasiparticle pole.

they always decay so quickly to more complicated states that they are of no practical significance. In fact, Landau's Fermi liquid theory is based upon the quasiparticle picture and as shown in Chapter 6 can provide an exact description of physical Fermion systems in an appropriate limit. The essential point can be seen simply by calculating the lifetime from the imaginary part of Σ_2 in Eq. (5.60). Since by the usual argument with outgoing wave boundary conditions, a state with complex energy $E = E_R - i\frac{\Gamma}{2}$ has lifetime $\tau = \frac{1}{\Gamma}$, the lifetime for a quasiparticle state α evaluated at the quasiparticle pole ϵ_α above the Fermi energy, *i.e.*, $\epsilon_\alpha > 0$, is given by

$$\frac{1}{\tau} = -2\,\mathrm{Im}\,\Sigma_2(\alpha, \epsilon_\alpha) = \frac{1}{2}\sum_{abB} |\{\alpha B|v|ab\}|^2\, 2\pi\delta(\epsilon_\alpha + \epsilon_B - \epsilon_a - \epsilon_b). \tag{5.70}$$

Note that if we had considered a hole state, the two-hole one-particle component of Σ_2 would have contributed instead of the two-particle one-hole component.

When the energy ϵ_α is close to the Fermi energy ϵ_F, phase space restrictions on the sum over a, b, and B severely limit the contributions to $\frac{1}{\tau}$. With the convention of measuring energies relative to ϵ_F, $\epsilon_B < 0$ and ϵ_α, ϵ_a, $\epsilon_b > 0$ so that the energy conservation condition in Eq. (5.70) is $\epsilon_\alpha = |\epsilon_a| + |\epsilon_b| + |\epsilon_B|$. Thus, neither ϵ_a nor ϵ_b may be greater than ϵ_α. Hence, letting $\rho(\epsilon)$ denote the density of states and defining the maximum values of $\rho(\epsilon)$ and $|\{\alpha B|\, v\,|ab\}|$ for $0 < \epsilon_a, \epsilon_b, |\epsilon_B| < \epsilon_\alpha$ as $\rho_{\max}$ and $V_{\max}$ we obtain the bound

$$\begin{aligned}\frac{1}{\tau} &\le \pi V_{\max}^2 \int_0^\infty d\epsilon_a \int_0^\infty d\epsilon_b \int_0^{-\infty} d\epsilon_B\, \rho(\epsilon_a)\rho(\epsilon_b)\rho(\epsilon_B)\delta\left(\epsilon_\alpha + \epsilon_B - \epsilon_a - \epsilon_b\right) \\ &= \pi V_{\max}^2 \int_0^{\epsilon_\alpha} d\epsilon_a \int_0^{\epsilon_\alpha} d\epsilon_b\, \rho(\epsilon_a)\rho(\epsilon_b)\rho\left(\epsilon_a + \epsilon_b - \epsilon_\alpha\right) \\ &\le \pi V_{\max}^2 \rho_{\max}^3 \epsilon_\alpha^2.\end{aligned} \tag{5.71}$$

No matter how strong the two-body interaction, as long as its matrix elements and the density of states remain finite in the vicinity of the Fermi surface, $\frac{1}{\tau}$ is therefore bounded by a constant times ϵ_α^2. A completely analogous argument holds for a quasi-hole. So in general, as the energy ϵ of a quasiparticle or quasi-hole excitation approaches the Fermi Energy ϵ_F, the lifetime increases as

$$\tau(\epsilon) \propto |\epsilon - \epsilon_F|^{-2}. \tag{5.72}$$

Thus, under very general conditions, a strongly-interacting many-Fermion system will always have a domain sufficiently close to the Fermi surface in which quasiparticles have arbitrarily long lifetimes and are the appropriate degrees of freedom to describe the system. Note that nowhere in this argument have we invoked momentum conservation, as in most common derivations, so this result is clearly applicable to finite systems and non-translationally invariant systems.

EFFECTIVE MASSES

We now consider the effect of the energy and momentum dependence of the self-energy on quasiparticle propagation in an interacting Fermi system. Whereas the analysis pertains to a variety of interesting physical systems, such as a ^{3}He atom in liquid ^{3}He or a low energy nucleon propagating in a nucleus, we will illustrate the major points for the case of a nucleon in translationally invariant nuclear matter.

From the dispersion relation defining the quasiparticle pole

$$\epsilon = \frac{k^2}{2m} + \Sigma(k, \epsilon) \tag{5.73}$$

the density of states may be calculated as follows

$$\begin{aligned}\frac{d\epsilon}{dk} &= \frac{k}{m} + \frac{\partial\Sigma}{\partial k} + \frac{\partial\Sigma}{\partial\epsilon}\frac{d\epsilon}{dk} \\ &= \frac{k}{m}\left(1 + \frac{m}{k}\frac{\partial\Sigma}{\partial K}\right)\left(1 - \frac{\partial\Sigma}{\partial\epsilon}\right)^{-1}.\end{aligned} \tag{5.74a}$$

It is often convenient to subsume the complicated effect of the medium on a particular process into a suitably defined effective mass. The density of states may thus be expressed

$$\begin{aligned}\frac{d\epsilon}{dk} &= \frac{k}{m^*} \\ m^* &\equiv m\left(1 + \frac{m}{k}\frac{\partial\Sigma}{\partial k}\right)^{-1}\left(1 - \frac{\partial\Sigma}{\partial\epsilon}\right).\end{aligned} \tag{5.74b}$$

Noting that m^* itself is the product of factors associated with the energy and momentum dependence of $\Sigma(k, \omega)$ it is useful to define the additional effective masses m_ϵ and m_k as follows (Jeukenne, Lejeune, and Mahaux 1976)

$$\begin{aligned}\frac{m_\epsilon}{m} &\equiv \left(1 - \frac{\partial\Sigma}{\partial\epsilon}\right) \\ \frac{m_k}{m} &\equiv \left(1 + \frac{m}{k}\frac{\partial\Sigma}{\partial k}\right)^{-1} \\ \frac{m^*}{m} &= \frac{m_\epsilon}{m} \times \frac{m_k}{m}\end{aligned} \tag{5.75}$$

and to study m_ϵ and m_k separately. Note that the factor $\frac{m}{m_\epsilon}$ is just the residue of the quasiparticle pole discussed in the last section.

The mass m_k reflects the spatial nonlocality of Σ, and may be understood qualitatively by considering the non-locality of the exchange term of the Hartree-Fock potential. As shown in Problem. 5.3, the general result for the exchange terms assuming a central potential $v(r)$ and spin degeneracy 2S+1 may be evaluated with plane wave states to obtain

$$\begin{aligned}\Sigma_1^{\mathrm{exch}}(k) &= -\frac{1}{2S+1}\sum_{|k'|<k_f} \langle kk'|v|k'k\rangle \\ &= -\frac{1}{2S+1}\int d^3r\; e^{ik\cdot r} v(r)\frac{3j_1(k_F r)\rho}{k_F r}.\end{aligned} \tag{5.76}$$

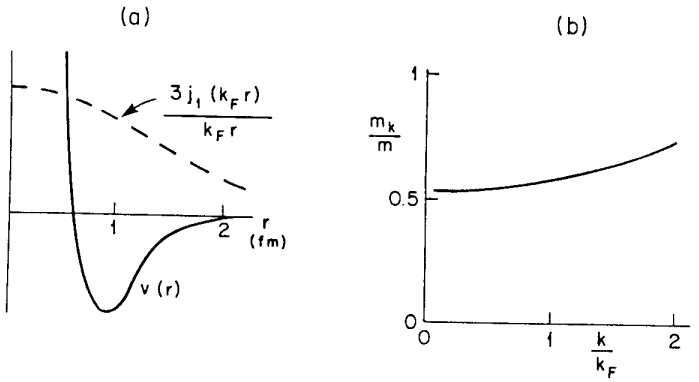

Fig. 5.8 Effective mass m_k in nuclear matter. Sketch (a) shows the two factors contributing to the Fourier transform of $\Sigma_1^{\rm exch}(k)$ in Eq. (5.77). The resulting effective mass $\frac{m_k}{m} = \left(1 + \frac{m}{k}\frac{\partial\Sigma}{\partial k}\right)^{-1}$ is shown in (b).

Note that a central potential contributes to the exchange term with the opposite sign and a strength reduced by $\frac{1}{2S+1}$. If the potential is state-dependent, then different combinations of partial waves contribute to the direct and exchange terms. In particular, if we consider nucleons with two internal degrees of freedom, spin and isospin, and assume even partial waves interact with a potential $v_{\rm even}$ and odd partial waves interact with the potential $v_{\rm odd}$, then, from Problem 5.3, the exchange term is

$$\Sigma_1^{\rm exch}(k) = \int d^3r\, e^{ik\cdot r}\left[\frac{3}{8}v_{\rm even}(r) - \frac{5}{8}v_{\rm odd}(r)\right]\frac{3j_1(k_F r)}{k_F r} \quad . \tag{5.77}$$

Since the nucleon-nucleon interaction is strongly attractive in even partial waves and weakly repulsive in odd partial waves, the effective potential

$$v_{\rm exch}(r) \equiv \frac{3}{8}v_{\rm even}(r) - \frac{5}{8}v_{\rm odd}(r) \tag{5.78}$$

contributing to the exchange integral is strikingly different than in the state-independent case. Both contributions to $v_{\rm exch}(r)$ are attractive, so that the net attraction from the exchange term is larger than from the direct term, and the qualitative behavior of $v_{\rm exch}(r)$ and the Slater density $\frac{3j_1(k_F r)}{k_F r}$ are sketched in Fig. 5.8a. Since $\sum_1^{\rm exch}(k)$ is given by the Fourier transform of the product of these two factors, its momentum dependence is obvious. At low k, $\Sigma(k)$ is strongly attractive and when $k >> k_F$, the characteristic scale in the integrand, $\Sigma(k) \to 0$. Hence $\frac{\partial\Sigma(k)}{\partial k}$ is a positive decreasing function of k, so that $\frac{m_k}{m} = \left(1 + \frac{m}{k}\frac{\partial\Sigma(k)}{k}\right)^{-1}$ has the behavior sketched in Fig. 5.8b. Note that at low momentum, the spatial nonlocality reduces m_k to roughly half of the bare mass m.

The mass m_ϵ reflects the nonlocality of Σ in time. Since the Hartree-Fock contribution to Σ is instantaneous, the leading contribution to m_ϵ arises from Σ_2, Eq.

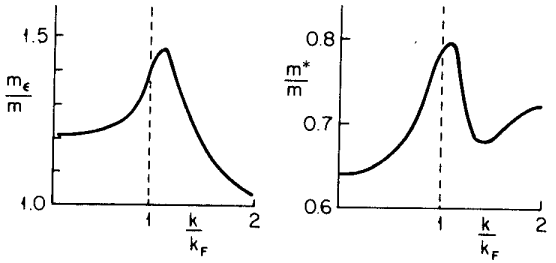

Fig. 5.9 Effective masses m_ϵ and m^* in nuclear matter.

(5.60). The qualitative behavior of this contribution may be understood by the following schematic argument (Bertsch and Kuo 1968). Represent the sum over all two-particle one-hole states by a single average state with excitation energy $\epsilon_a + \epsilon_b - \epsilon_B \sim E_x$ and an effective coupling matrix element V:

$$\Sigma_2^{2p1h}(k,\epsilon) = \frac{1}{2}\sum_{abB}\frac{|\{kB|v|ab\}|^2}{\epsilon + \epsilon_B - \epsilon_a - \epsilon_b} \approx \frac{1}{2}\frac{V^2}{\epsilon - E_x} \quad . \tag{5.79a}$$

Similarly, represent the sum over two-hole one-particle states by a single average state, and further assume that near the Fermi surface particle and hole states are symmetric. Then, $\epsilon_A + \epsilon_B - \epsilon_a \sim -E_x$ and

$$\Sigma_2^{2h1p}(k,\epsilon) = -\frac{1}{2}\sum_{ABa}\frac{|\{ka|v|AB\}|^2}{\epsilon_A + \epsilon_B - \epsilon_a - \epsilon} \approx \frac{1}{2}\frac{V^2}{\epsilon + E_x} \quad . \tag{5.79b}$$

Thus, both terms in Σ_2 become more negative as ϵ is increased from 0, yielding the following enhancement in m_ϵ at the Fermi surface.

$$\left.\frac{m_\epsilon}{m}\right|_{\epsilon_F} = 1 - \frac{\partial\Sigma}{\partial\epsilon} \approx 1 - \frac{d}{d\epsilon}\frac{1}{2}\left[\frac{V^2}{\epsilon - E_x} - \frac{V^2}{\epsilon + E_x}\right]_{\epsilon=0} = 1 + \frac{2V^2}{E_x{}^2} \quad . \tag{5.80}$$

This schematic analysis is too crude to calculate m_ϵ away from the Fermi surface, but detailed calculations (Jeukenne, Lejeune, and Mahaux, 1976) yield the behavior graphed in Fig. 5.9a. The enhancement is very large at the Fermi surface, of the order 50%, and falls off significantly away from the Fermi surface. The combined effect of m_ϵ and m_k in the total effective mass m^* measured in the density of states has the structure shown in Fig. 5.9b. Note that because m_k is so small, on the average m^* is significantly less than m. However, near the Fermi surface, the peak in m_k brings m^* nearly up to m.

Although the product of m_ϵ and m_k appears in the density of states, other observables depend on m_ϵ and m_k separately. Consider, for example, the mean free path, which is calculated by specifying a real energy ϵ, and solving the dispersion relation (5.74) for a complex k. Denoting the real and imaginary parts of Σ by U and W, k is given by:

$$\epsilon = \frac{k^2}{2m} + U(k,\epsilon) + iW(k,\epsilon) \quad . \tag{5.81}$$

Since the imaginary part W is small, it is sufficient to expand to first order in W about the zeroth-order solution k_0 given by

$$\epsilon = \frac{k_0^2}{2m} + U(k_0, \epsilon) \quad . \tag{5.82}$$

Writing $k \equiv k_R + ik_I$ and expanding Eq. (5.81) to first order, we obtain

$$\begin{aligned} \epsilon = & \frac{k_0^2 + 2k_0(k_R - k_0 + ik_I)}{2m} + U(k_0, \epsilon) \\ & + \left.\frac{\partial U}{\partial k}\right|_{k_0} (k_R - k_0 + ik_I) + iW(k_0, \epsilon) \end{aligned} \tag{5.83}$$

with the result

$$\begin{aligned} k_R &= k_0 \\ k_I &= -W(k_R, \epsilon)\left(\frac{k_R}{m} + \frac{\partial U}{\partial k}\right)^{-1} \\ &= -\frac{m_k}{k_R} W(k_R, \epsilon) \quad . \end{aligned} \tag{5.84}$$

Since the attenuation factor for a complex wave vector is $\psi_k^2 \sim \left|e^{i(k_R + ik_I)\cdot r}\right| \sim e^{-2k_I r}$, the mean free path is

$$\lambda = \frac{1}{2k_I} = -\frac{k_R}{2m_k W(k_R, \epsilon)} \tag{5.85}$$

and is thus proportional to $\frac{1}{m_k}$.

Similarly, the lifetime of a quasiparticle excitation is obtained by specifying a real k and solving for the complex energy. The zeroth order equation is

$$\epsilon_0 = \frac{k^2}{2m} + U(k, \epsilon_0) \tag{5.86}$$

and writing $\epsilon = \epsilon_R - \frac{i\Gamma}{2}$ we obtain

$$\begin{aligned} \epsilon_R - \frac{i\Gamma}{2} = & \frac{k^2}{2m} + U(k, \epsilon_0) \\ & + \left.\frac{\partial U}{\partial \epsilon}\right|_{\epsilon_0} \left(\epsilon_R - \epsilon_0 - i\frac{\Gamma}{2}\right) + iW(k, \epsilon_0) \end{aligned} \tag{5.87}$$

with the solution

$$\begin{aligned} \epsilon_R &= \epsilon_0 \\ \Gamma &= -2W(k, \epsilon_0)\left(1 - \frac{\partial U}{\partial \epsilon}\right)^{-1} = -2W(k, \epsilon_0)\frac{m}{m_\epsilon} \quad . \end{aligned} \tag{5.88}$$

Thus, the lifetime $\tau = \frac{1}{\Gamma}$ is proportional to m_ϵ. The two results for λ and Γ in Eqs. (5.85) and (5.88) are consistent since λ and Γ are related through the group velocity v:

$$\begin{aligned} \lambda &= \frac{v}{\Gamma} \\ v &= \frac{dE}{dk} = \frac{k}{m^*} = \frac{k}{m}\,\frac{m}{m_k}\,\frac{m}{m_\epsilon} \quad . \end{aligned} \tag{5.89}$$

The effective masses play a quantitatively significant role in determining the mean free path of a nucleon in the nuclear medium and serve to resolve a long-standing discrepancy with experiment. The mean free path in a nucleus of neutrons in the energy range 50 – 150 MeV may be determined from the amplitude of shape resonances in total neutron scattering cross sections. In this analog of the atomic Ramsauer effect, interference between the incident and transmitted wave can only be observed if the mean free path is long enough for a neutron to pass through the nuclear medium, and in this way one measures $\lambda \sim 6\,\text{fm}$ for neutrons in this energy regime (Bohr and Mottelson, 1969).

The naive classical estimate of a mean free path $\lambda = \frac{1}{\bar{\sigma}\rho}$ which ignores the Pauli principle is far too low, with the average nucleon-nucleon cross section at 100 MeV $\bar{\sigma} = 5.5\,\text{fm}^2$ and nuclear density $\rho = 0.16\,\text{fm}^{-3}$yielding $\lambda = 1.1\,\text{fm}$. The simplest approximation to $W = \text{Im}\,\Sigma$ is obtained from Eq. (5.70) by replacing matrix elements of the potential $\{kB|v|ab\}$ by the free space T-matrix $\{kB|T|ab\}$ measured experimentally and replacing the energies ϵ_α in the medium by the free space energies $\frac{k_\alpha^2}{2m}$:

$$W^T(k, \epsilon) = -\frac{\pi}{2}\sum_{abB} |\{kB|T|ab\}|^2\, \delta\left(\epsilon + \frac{k_B^2}{2m} - \frac{k_a^2}{2m} - \frac{k_b^2}{2m}\right) \quad . \tag{5.90}$$

Using this estimate for W and ignoring the effective mass in Eq. (5.85) yields $\lambda = -\frac{k}{2mW^T} \sim 3\,\text{fm}$, still far short of the experimental result of 6 fm. Thus, simply including the Pauli principle through the restriction $ab > k_F$, $B < k_F$ is insufficient. However, this formula omits two effective mass factors. The δ-function in (5.90) with free propagators simply includes the free Fermi gas density of states. Since the δ-function in Σ, Eq. (5.70), contain the energies in the medium, W^T should be multiplied by $\frac{m^*}{m}$ to include the density of states in the medium. Including the additional factor of m_k from Eq. (5.85), the correct T-matrix expression for the mean free path is

$$\lambda = -\left(\frac{m}{m_k}\right)\left(\frac{m}{m^*}\right)\frac{k}{2mW^T} \sim 6\,\text{fm} \quad . \tag{5.91}$$

Thus, the medium dependence reflected in the two effective mass factors, each of the order of $\sim \frac{1}{0.7}$ is crucial to understanding the nucleon mean free path (Negele and Yazaki 1981, Fantoni, Friman and Pandharipande 1981).

OPTICAL POTENTIAL

Another important physical property of the self-energy is the fact that it specifies the optical potential for the scattering of a particle from a composite system made up of identical particles (Bell and Squires 1959).

Consider the elastic scattering of an electron from an atom or a nucleon from a nucleus. Since the composite system is required to remain in its ground state, the asymptotic scattering state may be described by a wave function $\phi(r)$ depending only on the relative coordinate between the composite system and the scattered particle. By definition, the optical potential is a one-particle potential producing phase shifts identically equal to those produced in $\phi(r)$ for the full many-body problem. Note that since any phase-shift equivalent potential is satisfactory, the optical potential is not unique.

The essential point in relating the optical potential to the self-energy is the observation that the wave function can be written in terms of the one-particle Green's function. Since $G(rt|r't')$ is the amplitude for adding a particle to a system at $r't'$ and detecting it at rt, it is clear that we should be able to express the scattering wave function in terms of G. To be precise, let $|\psi\rangle$ be the ground state of the N-body composite system and pick the zero of the energy scale such that its energy is zero. Then a scattering state may be generated by creating a particle at some point r' far away from the system at time t' and projecting onto a specific energy E by integrating over initial times

$$|S\rangle = \int dt'\, e^{-iEt'} \left[\theta(t'-t) + \theta(t-t')e^{-iH(t-t')}\psi^\dagger(r')\right]|\psi_0\rangle \ . \tag{5.92}$$

Since the optical model wave function is the amplitude for observing one particle at r and all other particles in the ground state $|\psi_0\rangle$, we obtain

$$\begin{aligned}\phi(\vec{r},t) &= \langle 0|\hat{\psi}(r)|S\rangle \\ &= \int dt'\, e^{-iEt'}\langle\psi_0|\theta(t-t')e^{iHt}\hat{\psi}(r)e^{-iHt}e^{iHt'}\hat{\psi}(r')e^{-iHt'}|\psi_0\rangle \qquad (5.93)\\ &= \int dt' e^{-iEt'}\langle\psi_0|\theta(t-t')\hat{\psi}(r,t)\hat{\psi}^\dagger(r',t') - \theta(t'-t)\hat{\psi}^\dagger(r',t')\hat{\psi}(r,t)|\psi_0\rangle \\ &= e^{-iEt}iG(E;r,r') \ .\end{aligned}$$

In the second line, we have used the fact that the $\theta(t'-t)$ term in (5.92) does not contribute because $\langle 0|\psi(r)|0\rangle = 0$ and have inserted exponentials next to $|\psi_0\rangle$ because $H|\psi_0\rangle = 0$. The second time order in the third line required to obtain the Green's function could be inserted because $\langle 0|\hat{\psi}^\dagger(r',t') = (\psi(r',t')|0\rangle)^\dagger = 0$ since r' is far from the target and there are thus no particles for ψ to annihilate. For convenience, we will evaluate the wave function at time $t=0$ and drop the factor i so that $\phi(r) = G(E;r,r')$.

Consider, for reference, the problem in which the interacting Hamiltonian H is replaced by $H_0 = T + U$, where U is a one-body potential (such as the Hartree-Fock potential) producing a first approximation to the localized N-body target. Then, by the previous argument, scattering from the one-body potential U is described by the wave function $\phi_0(r) = G_0(E;r,r')$. Substituting $\phi(r)$ and $\phi_0(r)$ in the Dyson equation $G = G_0 + G_0\Sigma G$, we may write

$$\phi(r) = \phi_0(r) + \int dr''dr'''\, G_0(E;r,r'')\Sigma(E;r'',r''')\phi(r''') \ . \tag{5.94a}$$

Note from the spectral representation for G_0, Eq. (5.29), that for the positive energies relevant to the scattering problem the denominator in the $(N+1)$ particle term never vanishes so that $G_0(E)$ may be replaced by the retarded Green's function $G_0^R(E)$ having $E+i\eta$ in both terms. Thus, we may rewrite Eq. (5.94a) in the form

$$|\phi^+\rangle = |\phi_0^+\rangle + \frac{1}{E^+ - T - U}\Sigma|\phi^+\rangle \tag{5.94b}$$

where $|\phi^+\rangle$ and $|\phi_0^+\rangle$ denote the scattering wave function for the interacting and non-interacting problems $\phi(r)$ and $\phi_0(r)$ and $E^+ \equiv E + i\eta$. Because $|\phi_0^+\rangle$ is the scattering wave function for the potential U, it satisfies the Lippmann-Schwinger equation

$$|\phi_0^+\rangle = |\phi_0\rangle + \frac{1}{E^+ - T}U|\phi_0^+\rangle \tag{5.95}$$

where $|\phi_0\rangle$ denotes an incident plane wave. Substituting $|\phi_0^+\rangle$ from Eq. (5.94b) into (5.95) we obtain the desired Lippmann-Schwinger equation for $|\phi^+\rangle$

$$|\phi^+\rangle = |\phi_0\rangle + \frac{1}{E^+ - T}(U+\Sigma)|\phi^+\rangle \tag{5.96}$$

so that the optical potential is $U + \Sigma$.

When the self-energy is expanded in $H - H_0 = \frac{1}{2}\sum_{ij} v(r_i - r_j) - U$, the first order term containing $-U$ exactly cancels U and the first few time-ordered contributions to the optical potential are

$U + \Sigma =$ 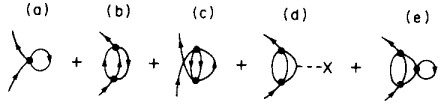

(5.97)

Diagram (a) describes propagation in the Hartree-Fock mean field and (b) represents the amplitude for coupling to a two-particle one-hole state and propagating in that state rather than in the single-particle state. Diagram (c) expresses the fact that in the interacting system, two normally occupied states A and B may be virtually excited to states a and k, thus blocking the addition of a particle in state k to the system. In contrast to other approaches to multiple scattering theory in which antisymmetry is either neglected or put in laboriously by hand, the self-energy systematically includes its effects through terms such as this. Diagrams (d) and (e) are representative of an infinite class of terms in which U and the Hartree-Fock potential enter with opposite signs. As usual, it is advantageous to cancel such terms identically by choosing U to be the Hartree-Fock potential.

Because one-particle irreducibility is defined in terms of Feynman diagrams rather than time-ordered diagrams, both of the following time-ordered diagrams are excluded from the optical potential

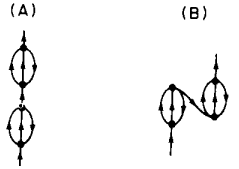

(5.98)